

**Ventilation for Energy Efficiency and Optimum
Indoor Air Quality
13th AIVC Conference, Nice, France
15-18 September 1992**

Paper 6

**Modelling Fluctuating Airflow Through Large
Openings.**

F. Haghightat^{*}, J.Rao^{*}, J. Riberon^{}**

*** Centre for Building Studies, Concordia
University, 1455 de Maisonneuve Blvd. W.,
Montreal, Canada.**

**** CSTB (Centre Scientifique et Technique du
Bâtiment) 02-77421 Marne La Vallée, France.**

SYNOPSIS

Fluctuating airflow through buildings is caused by temporal and spatial variations of wind-induced pressures around building envelopes, and include pulsating airflow and eddy penetrations. Two approaches using a multi-zone pulsating airflow model are introduced in this paper to study the eddy penetration and multi-way airflow through large openings. In the first approach, the eddy flow is considered to be caused by imperfect correlations among pressures at different points of an opening. The concept of aerodynamic admittance functions is employed to modify the wind pressure spectra to represent the net effect of fluctuating pressures over the area of the opening. The other approach considers a large opening as composed of a number of smaller airflow paths, each permitting only pulsating airflow. Theoretical solutions are compared with field experimental results from the BOUIN test-house at CSTB, France.

LIST OF SYMBOLS

A_1, L_1, A_2, L_2 : effective opening areas and opening depths,

K_1, n_1, K_2, n_2 : power law coefficients and exponents,

$\bar{P}_1^w, \bar{P}_2^w, \bar{P}^i, \bar{Q}_1, \bar{Q}_2$: mean values of wind-induced pressures, internal pressure and airflow rates ,

$P_1^w(t), P_2^w(t), P^i(t), q_1(t), q_2(t), q^i(t)$: fluctuating components of wind pressures, internal pressure, airflow through openings, and compressibility airflow,
 f, ω : frequency and angular frequency, $f = 2\pi\omega$

$P_1^w(\omega), P_2^w(\omega), P^i(\omega), Q_1(\omega), Q_2(\omega), Q^i(\omega)$: Fourier transform of corresponding variables,

$S_{P_1^w}(\omega), S_{P_2^w}(\omega), S_{P_1^w P_2^w}^{(c)}(\omega), S_{P^i}(\omega)$: spectra and co-spectrum of two wind-induced pressures, and internal pressure spectrum,

$H_{P^i P_1^w}(\omega), H_{P^i P_2^w}(\omega)$: transfer functions between external and internal pressure,

$\chi_1(\omega)$: aerodynamic admittance function,

ρ air density, P_a atmosphere pressure, $\gamma=1.4, j = \sqrt{-1}$.

1. INTRODUCTION

Airflow through openings in building envelopes and internal walls is caused by the combined effects of three driving forces: wind-induced pressures, thermal buoyancy and mechanical systems. This airflow can be divided into steady-state airflow and fluctuating airflow. Steady-state or mean airflow is generated by mean pressure differences due to driving forces. The primary unsteady variables that cause fluctuations in airflow are temporal variations in wind-induced pressures.

Fluctuating airflow through individual openings caused by temporal variations in pressure differences can be divided into two types: the pulsating flow and the penetration of eddies. The pulsating flow results from the wind fluctuation and the compressibility of air in the building internal space. Fluctuations in the wind causes simultaneous positive or negative pressure variations at an opening.

The inside air is thus either pressurized or depressurized. The eddy flow is due to the turbulence in the air stream. They create a rotational effect on the inside air. This leads to an exchange between the inside air and the outside air through openings.

A model has been developed for predicting pulsating airflow in multi-zone buildings [1,2]. Inputs to the model include: the building airflow system (rooms, openings, and connections), the frequency characteristics of wind-induced pressures and their correlations, and output from a steady-state airflow model. In this paper, this model is extended to account for the effect of eddy flow, and is compared to field experimental data.

2. BOUIN TEST HOUSE AT CSTB, FRANCE

Field experiments were conducted in France by CSTB to study single sided ventilation [3]. The test house at Bouin (Figure 1a) was a single zone building on an exposed site near the Atlantic coast. The volume of the test house was 93.6 m^3 . The equivalent air leakage area of the house was measured and was less than 5 cm^2 . The building was mounted on a turntable that can be rotated during an experiment.

A sharp edged slot of 40 cm wide, 2.5 cm high and 1 cm thick was located in the building envelope. During the experiment, this opening was positioned to face the wind direction. The wind-induced external pressures, internal pressures, wind speed and direction, and tracer gas concentration were measured simultaneously at a rate of 10 Hz.

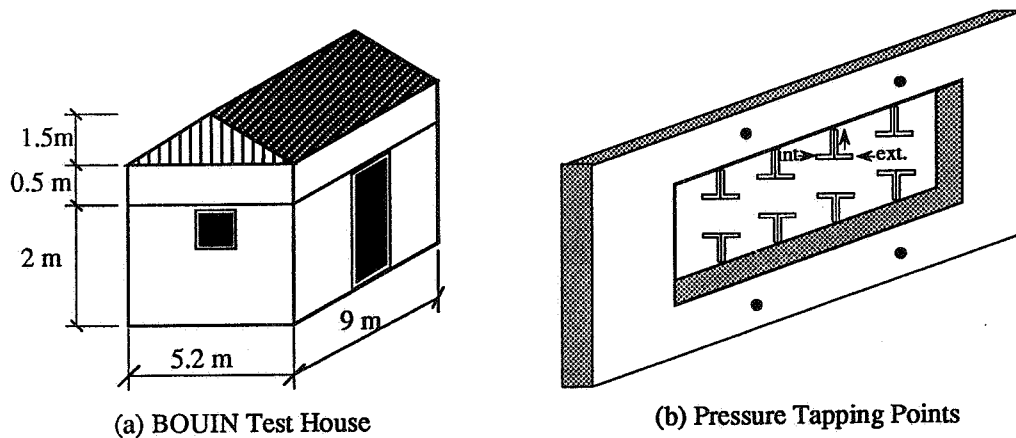


Figure 1. BOUIN Test House and Slot Opening

The wind pressure was measured close to the opening. This pressure was equal to the difference between the total pressure and the external static pressure. The pressures were also measured at eight points within the opening (Figure 1b), both inside and outside the building, allowing the direction of flow to be known locally. Full details of the site and the measurement used can be found in Riberon and Villain [4].

3. PULSATING AIRFLOW MODEL

In the pulsating airflow model presented in [1,2], the analysis is performed in the frequency domain. The task of calculating the pulsating airflow due to temporal variations in wind-induced pressures is decomposed into an infinite series of simple problems. Each problem calculates the corresponding portion of airflow caused by the simple sine wave pressure at a single frequency. The total airflow is then obtained by summing up all these infinitesimal portions of airflow at single frequencies. The formulation procedure for nodal governing equations of fluctuating airflow is demonstrated in the following using the BOUIN test house as an example.

In the steady-state calculation, the test house is modelled as a single-zone building with two openings. Opening 1 is the purpose-provided slot opening, and opening 2 represents the total leakage of the house envelope (Figure 2). The air mass balance for this building is written as:

$$K_1(\bar{P}_1^w - \bar{P}^i)^{n_1} + K_2(\bar{P}_2^w - \bar{P}^i)^{n_2} - 0 \quad (1)$$

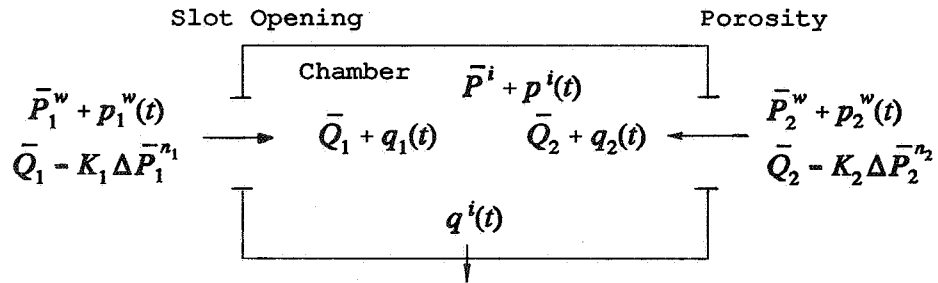


Figure 2. Modelling BOUIN House

For fluctuating airflow through the openings, the pressure differences are balanced by the forces required to overcome the flow resistance and the inertia of air in the openings, i.e.:

$$K_i^{-\frac{1}{n_i}} \left\{ (\bar{Q}_i + q_i)^{\frac{1}{n_i}} - \bar{Q}_i^{\frac{1}{n_i}} \right\} + M_i \frac{dq_i}{dt} = p_i^w - p^i \quad (2)$$

where $M_i = \rho L_i / A_i$, the subscripts $i = 1, 2$ and is the same for the following equations.

The nonlinear terms in the above equations are approximated to linear relations using a statistical linearization method. The linear fluctuating airflow equation for the openings can be expressed as:

$$M_i \frac{dq_i}{dt} + \lambda_i q_i = p_i^w - p^i \quad (3)$$

The coefficients λ_i are assigned to values such that the statistical variances of the nonlinear terms and the linear relations are the same. Equation (3) is then Fourier transformed into the frequency domain, and the fluctuating airflow equations in the frequency domain can be expressed as:

$$Q_i(\omega) = \frac{1}{\lambda_i + j\omega M_i} [p_i^w(\omega) - P^i(\omega)] \quad (4)$$

The compressibility of air in the room influences the fluctuating airflow through the building. The air mass increments due to pressurizations of the air volume in the building and decrements due to depressurizations are modelled by an imaginary airflow path which connects the room with the atmosphere. This compressibility airflow, $q^i(t)$, is related to the fluctuating internal pressure by:

$$p^i(t) = -\frac{\gamma P_a}{V} \int_0^t q^i(v) dv = -B \int_0^t q^i(v) dv \quad (5)$$

Applying a Fourier transformation, the fluctuating airflow equation for the imaginary compressibility airflow path can be written in the frequency domain as:

$$Q^i(\omega) = -\frac{j\omega}{B} P^i(\omega) \quad (6)$$

The airflow system of the BOUIN house, therefore, can be modelled by three openings in the frequency domain: the purpose provided slot opening, the porosity, and the imaginary airflow path for air compressibility. The governing equation can be obtained from the air mass balance:

$$Q_1(\omega) + Q_2(\omega) - Q^i(\omega) = 0 \quad (7)$$

Applying fluctuating airflow equations (4 & 6), the governing equation with the internal pressure as the unknown variable is obtained. Transfer functions for the internal pressure can be calculated as:

$$H_{p^i}(\omega) = \frac{P^i(\omega)}{P_i^w(\omega)} = \left\{ \frac{1}{\lambda_i + j\omega M_i} \right\} / \left\{ -\frac{j\omega}{B} + \sum_{i=1,2} \frac{1}{\lambda_i + j\omega M_i} \right\} \quad (8)$$

When the spectra and co-spectrum of the wind pressures are known, the spectrum for the fluctuating internal pressure is calculated by the spectral relation:

$$S_{p^i}(\omega) = \|H_{p^i1}\|^2 S_{p_1^w}(\omega) + \|H_{p^i2}\|^2 S_{p_2^w}(\omega) + 2\|H_{p^i1}\| \|H_{p^i2}\| S_{p_1^w p_2^w}^{(c)}(\omega) \quad (9)$$

In turn, the RMS (root-mean-square) value and other statistical information of the fluctuating internal pressure can be derived from the spectrum.

4. MODIFIED FLUCTUATING AIRFLOW MODEL

The mean and RMS values for variables of interest are displayed in Table 1. Figure 3 shows the magnitude and phase plots of the transfer function $H_{p^i}(\omega)$ for both experimental estimation and theoretical calculation based on the pulsating airflow model.

The discrepancy between theoretical and experimental results shown in Figure 3 can be attributed to the fact that the pulsating airflow model does not consider the eddy flow due to the spatial variations of wind pressures over the opening. The pressures on the area of the opening are assumed to be simultaneously pushing in or pulling out the air through the opening at all points. In reality, however, the pressures at different points on the opening are not perfectly synchronized or correlated due to the presence of eddies. Although these pressures have (or are assumed to have) the same statistical and stochastic properties, there are differences between these pressures. The differences are influenced by the distance between the two points, the turbulence characteristics, and eddy sizes.

Table 1. Experimental and Pulsating Airflow Model

| | | Experimental | | Theoretical | | |
|---------------------------------|---------------------------|--|------|-------------|------|---------------|
| | | Mean | RMS | Mean | RMS | Flow Reversal |
| Opening | | $K_1=7.6771 \times 10^{-3}$ $n_1=0.5$ | | input | | NA |
| Porosity | | $K_2=8.3424 \times 10^{-4}$ $n_2=0.5$ | | input | | NA |
| P_1^w | | 14.45 | 5.02 | input | | NA |
| P_2^w | | -4.35 | 1.51 | input | | NA |
| Pulsating Model | P^i (Pascal) | 13.60 | 4.53 | 14.23 | 4.72 | NA |
| | Q_1 (l/s) | 4.93 | 6.24 | 3.60 | 4.72 | 22.3% |
| | Q_2 (/s) | 3.02 | 0.59 | 3.60 | 0.66 | 0 |
| Aerodynamic Admittance Approach | P^i (Pascal) | 13.60 | 4.53 | 14.23 | 4.50 | NA |
| | Q_1 (l/s) | 4.93 | 6.24 | 3.60 | 5.17 | 24.3% |
| | Q_2 (m ³ /s) | 3.02 | 0.59 | 3.60 | 0.66 | 0 |
| Multi-Path Approach | P^i (Pascal) | 13.60 | 4.53 | 14.23 | 4.60 | NA |
| | Q_1 (l/s) | 4.93 | 6.24 | 3.60 | 5.50 | 25.7% |
| | Q_2 (l/s) | 3.02 | 0.59 | 3.60 | 0.31 | 0 |

Note: NA: not available or not applicable.

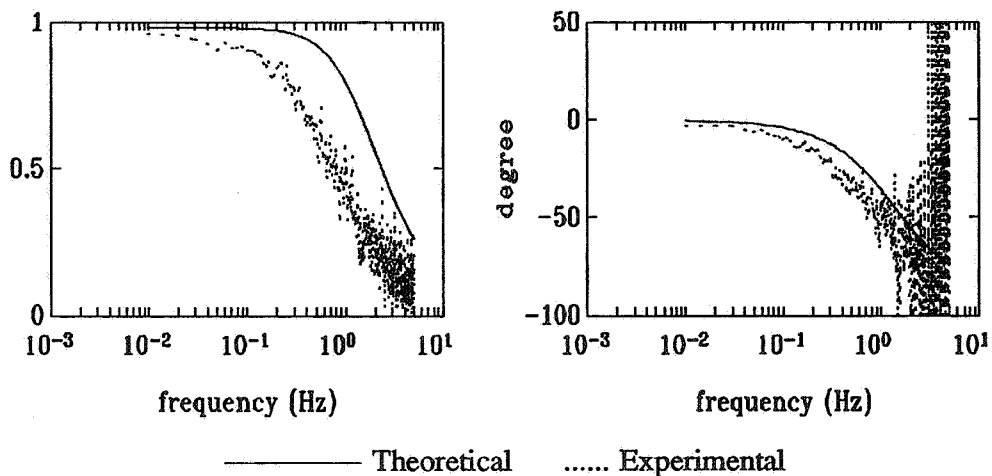


Figure 3. Results of Pulsating Model: (a) Magnitude and (b) Phase Plots of Transfer Function Between External and Internal Pressures

As a solution, a function is introduced to obtain the net effect of the imperfectly correlated pressures. Since the net force is always less than the "point" pressure (multiplied by the opening area), the function should be bounded from above by a value of 1. Because the differences are related to eddy sizes or the frequency, this function is related to the frequency. The concept of this function has been utilized in wind engineering to calculate the dynamic wind loading on building envelopes [5]. The function is referred to as an aerodynamic admittance function.

In the proposed approach to account for the eddies in the airflow through the opening, the aerodynamic admittance function is chosen to be the coherence function of wind-induced pressures at two representative points. Figure 4 shows the experimental estimation of the coherence function and fitting. The fitting curve will be used for later calculation.

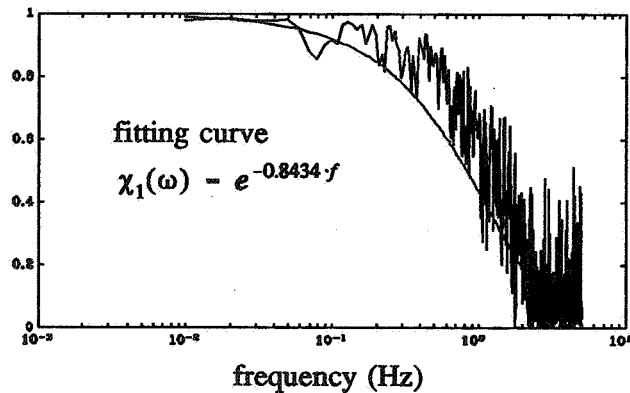


Figure 4. Coherence Function as Aerodynamic Admittance Function

Once the aerodynamic admittance function is obtained, the net effect should equal to the "point" value modified (multiplied) by the aerodynamic admittance function. In the theoretical calculation the "point" force is the power spectrum of the external pressure at the opening. Therefore, the calculation will take:

$$\hat{S}_{p_1^*}(\omega) = S_{p_1^*}(\omega) \cdot \chi_1^2(\omega) \quad (10)$$

as the input force. A further analysis shows this is equivalent to using a modified transfer function:

$$\hat{H}_{p_1^*}(\omega) = H_{p_1^*}(\omega) \cdot \chi_1(\omega) \quad (11)$$

in the theoretical calculation.

The comparison between experimental estimations and theoretical calculations by the modified model is shown in Figure 5. The plots show an improvement of the modified model over the pulsating model in predicting the transfer function. Table 1 also shows that the predicted RMS value of the internal pressure by the modified model is closer to the experimental results. The new approach also results in a larger RMS of airflow at the slot opening.

The second approach for modelling large openings is to consider airflow through an opening as composed of several separate airflows (sub-flows). Each sub-flow is a pulsating airflow and is modelled as one distinct airflow path using the pulsating airflow model. In this way, the limitation to pulsating airflow is overcome, and eddy flow or multi-way airflow through large openings can be accounted for in the prediction.

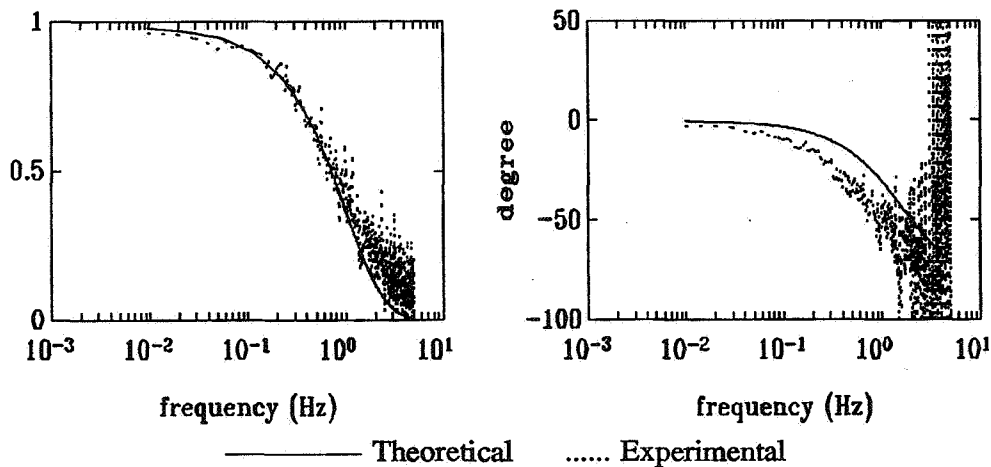


Figure 5. Results of Modified Model: (a) Magnitude and (b) Phase Plots of Transfer Function Between External and Internal Pressures

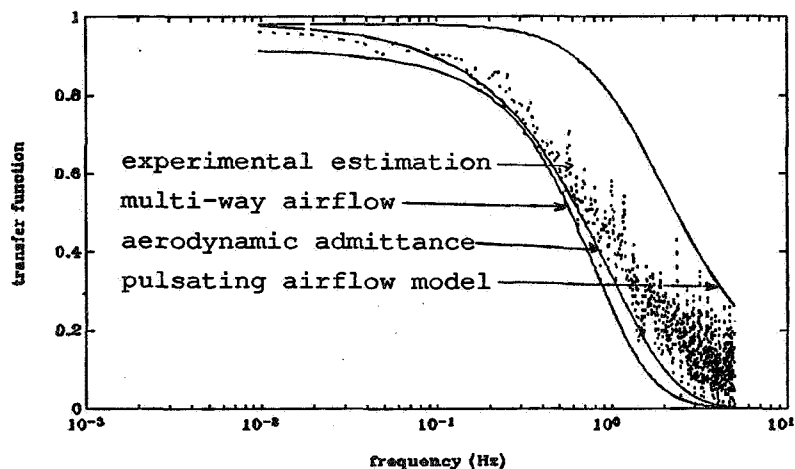


Figure 6. Results of Multi-Path Model: Magnitude Plot of Transfer Function Between External Pressure and Internal Pressure

The slot opening of the BOUIN house is modelled as two flow paths. The theoretical results based on this modified model is shown in Table 1 and Figure 6. The predictions of the transfer function and RMS value for the internal pressure, as well as for the fluctuating airflow, show an improvement over the original pulsating airflow model.

The total air exchange across an opening is determined by both the mean and fluctuating airflow rates. The amount of flow reversal due to contributions from fluctuating components can be calculated from the RMS values and by assuming normal distributions for the temporal variations in the airflow rates. The last column of Table 1 shows the percentage of fluctuating airflow that is involved in flow reversal through the slot opening. Let this percentage be β , the total air exchange across the opening is the summation of the mean airflow rate (\bar{Q}) and 3/2 of its fluctuating component (σ_q). Calculations (Table 2) show that due to fluctuations in the airflow, the air exchange across the slot opening is approximately 40 to 60 percent more than the mean value.

Table 2. Airflow Rate (l/s) Through Slot Opening

| | \bar{Q} | σ_q | β | $\bar{Q} + \frac{3}{2}\beta\sigma_q$ | $[\frac{3}{2}\beta\sigma_q]/\bar{Q}$ |
|------------------------|-----------|------------|---------|--------------------------------------|--------------------------------------|
| Pulsating | 3.60 | 4.72 | 0.223 | 5.18 | 43.9% |
| Aerodynamic Admittance | | 5.17 | 0.243 | 5.48 | 52.4% |
| Multi-Path | | 5.50 | 0.257 | 5.72 | 58.8% |

5. CONCLUSION

The pulsating airflow model and its modified versions for large openings perform analyses in the frequency domain, and take the spectra and co-spectra as input. The model provides predictions on statistical characteristics of the resultant airflow. The frequency analyses have the advantage of less computations over other models based on time domain simulations. The greater stability of the wind-induced pressure spectral information compared to the time signals also makes the model easier to apply in other general situations.

In accounting for fluctuating airflow through large openings, two approaches are employed. One approach utilizes the concept of aerodynamic admittance function. The net force that is pushing in or pulling out the air through the opening is considered to be the "point" pressure multiplied by the aerodynamic admittance function. The coherence function is chosen as the modifying function. The other approach considers airflow through a large opening as composed of multi-way flows and models the opening by several flow paths. The new approaches are applied to field experimental data from BOUIN test house in France. The comparison shows that both approaches are quite effective in explaining the experimental results.

References

1. Haghghat, F., Rao, J., and Fazio, P. (1991), "The Influence of Turbulent Wind on Air Change Rates - a Modelling Approach", *Building and Environment*, vol. 26, No. 2, pp. 95-109.
2. Rao, J. and Haghghat, F. (1991), "Wind Induced Fluctuating Airflow in Buildings", *Proc. of the 12th AIVC Conference*, Ottawa, Canada.
3. Bienfait, D., Phaff, H., Vandaele, L. Van der Maas, J. and Walker, R. (1991), "Single Sided Ventilation", *Proc. of the 12th AIVC Conference*, Ottawa, Canada, vol. 1, pp. 73-98.
4. Riberon, J. and Villain, J. (1990), "Etude en vraie grandeur des débits effectifs de renouvellement d'air", CSTB GEC/DAC-90.101R, Champs-Sur-Marne.
5. Simiu, E. and Scanlan, H. (1986), *Wind Effects on Structures - An Introduction to Wind Engineering*, Wiley, New York.

